Subsurface wireless chemical sensing strategy compatible with Ground Penetrating RADAR

J.-M Friedt, A. Hugeat, S. Lamare, F. Chérioux
Institut FEMTO-ST,
CNRS, Université Bourgogne Franche-Comté,
Besançon, France
Email: jmfriedt@femto-st.fr

D. Rabus, L. Arapan, S. Alzuaga
SENSeOR SAS, Besançon, France

***Abstract*—Ground Penetrating RADAR (GPR) is a suitable measurement candidate for the development of interrogative systems of passive buried transducers acting as cooperative targets in the field of sub-surface sensing. We address the compatibility of GPR for monitoring chemical compounds in soil or in the water table. This has been achieved by using a chemical sensor based on surface acoustic wave reflective delay lines interrogated by a GPR. As model target, we focus on hydrogen sulfide, which is a gas soluble in water causing health hazard and water pollution. After demonstrating the chemical functionalization of acoustic delay lines with a polymer designed for hydrogen sulfide detection through the specific reaction of sulfur with lead, we have successfully achieved the detection of hydrogen sulfide in air by GPR. We then consider extending this strategy towards sensors operating in liquid phase.**

Ground Penetrating RADAR (GPR) cooperative target design constraints [1], [2] have been described previously for addressing sub-surface identification [3] or sensing [4]. The requirements are summarized as delaying the echoes from the cooperative targets, representative of the quantity under investigation, beyond clutter, and maximizing the returned signal power at such a long delay. Such requirements are well met by surface acoustic wave (SAW) transducers whose delay and sensing mechanism is based on the conversion of the incoming electromagnetic pulse to an acoustic wave. This acoustic wave propagates at the air-substrate interface to reach a mirror (electrodes) patterned on the surface (Fig. 1). Then, the acoustic pulse propagates back through the sensing area to the interdigitated electrodes connected to the antenna and is converted back to an electromagnetic signal propagating towards the GPR receiver: from a user perspective, a SAW delay line is an electrical dipole delaying a signal by several microseconds in a compact package only a few millimeter long and exhibiting insertion losses in the 30 to 40 dB range.

Liquid phase sensing of sub-surface pollutant often addresses small molecule detection: most commonly, heavy metal, nitrate or phosphate pollution related to intensive agricultural activities, or volatile organic solvent [5], [6] are some of the most commonly tackled issues. However, detecting such small molecules in a direct detection sensor, in which the sensing layer must selectively react with one compound and prevent false alarm by reacting with unwanted compounds, is often challenging. Even in the case of heavier molecules such as pesticides, selective antibodies have been designed yet the resulting response remains minute due to the unfavorable balance between the heavy selective molecules – antibodies typically in the tens of kilodaltons – and the light pesticide – typically in the few tens to hundred dalton range.

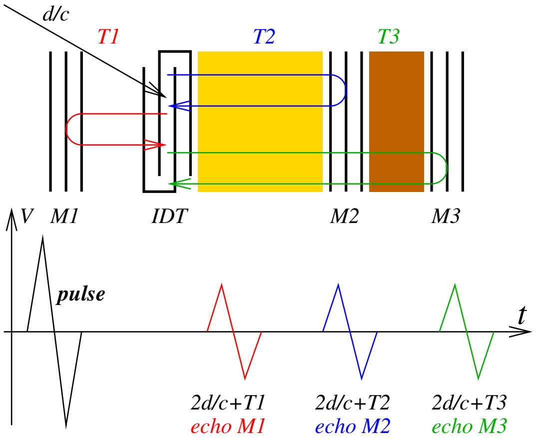

Fig. 1. Top: schematic principle (top view) of the delay line. The interdigitated transducer (IDT) converts the incoming electromagnetic pulse, after a propagation time d/c from the GPR unit located at distance d at a velocity c, to a surface acoustic wave. This wave propagates at the surface of the piezoelectric substrate until it meets electrodes acting as Bragg mirrors (Mi, $i \in [1..3]$) which reflect a fraction of the pulse power back to the IDT, re-emetting an electromagnetic pulse through direct piezoelectric effect. Each sensing area (between IDT and M1, IDT and M2, M2 and M3) is functionalized with a different chemical compound, inducing a different velocity shift when exposed to a given environment. Bottom: schematic of the returned signal: a differential measurement of time delay between pulses gets rid of the propagation duraction from the GPR to the sensor and allows extracting Ti individually.

Liquid-phase sub-surface sensing requires designing cooperative targets meeting multiple requirements: passive transducers probed through a wireless link exhibiting strong backscattered signals (i.e. high RADAR cross-section), and a transduction mechanism sensitive to the presence of a compound which is not significantly damped when exposed to liquid [5], [6]. Surface acoustic wave transducers have been demonstrated to meet the first requirements of passive wireless sensing, and are well known for chemical sensing once the surface of the transducer has been coated with a chemical layer selectively reacting when exposed to the compound to be detected [7],

[8], [9] . Indeed, the acoustic wave propagation velocity is dependent on boundary conditions which include adlayer mass (density times thickness): absorbing a chemical compound or varying the layer stiffness will induce an acoustic velocity variation readily detected as an echo time of flight variation.

While each one of these requirements has been independently demonstrated, combining in a single transducer the wireless chemical sensing capability compatible with compounds dissolved in a liquid have seldom been shown [10], [11], [12], [13]. The compatibility with GPR, which would open the way towards sub-surface pollutant detection with the classical geophysical instrument, has never been addressed.

We investigate the role of GPR as a new tool for sub-surface chemical sensing and highlight how appropriate acoustic transducters are as cooperative targets by focusing on the detection of a specific compound: hydrogen sulfide (H_2S). Hydrogen sulfide is of interest because its release appears as a health hazard [14] in oil and gas well exploitation [15], [16], as well as a promoter of corrosion [17] when associated with water. It is produced by anaerobic bacteria and is a pollutant in waste water as well [18], [19].

In this paper we consider four steps in sub-surface detection of hydrogen sulfide dissolved in water by GPR:

1) a strategy for detecting hydrogen sulfide with surface acoustic wave transducers,
2) functionalizing acoustic transducers with the hydrogen-sulfide selective compounds, which includes spreading homogeneously over the sensing surface a controlled thickness of the detecting compound,
3) probing the sensor with a GPR and extracting an information relevant of hydrogen sulfide concentration,
4) addressing the compatibility of sensing compounds in liquid phase.

Each one of these topics will be discussed and provide the layout of the discussion.

I. HYDROGEN SULFIDE DETECTION

SAW-based hydrogen sulfide detection has been addressed in [20] using a conductivity change effect: our approach differs in searching for a selective, non-reversible reaction of the gas with an appropriately designed detection layer. Following this strategy, chemical sensing requires a thin film adsorbed on the surface of the transducer, selectively reacting with the compound to be detected. A thin film is needed because on the one hand compound diffusion time is reduced if the film is thin enough for the diffusion time to be small with respect to the chemical reaction kinetic, and on the other hand the evanescent acoustic wave probing the thin film properties – namely acoustic velocity and losses related to its Young modulus, density and viscosity – only penetrates a few skin depths into the sensing layer. The skin depth δ is given by $\delta = \sqrt{\frac{\eta}{2\pi f\rho}}$ where ρ and η are the layer density and viscosity respectively: the skin depth is of the order of 40 nm in water and 150 nm in air for a device operating at $f = 100$ MHz. Additionally, this coating must act as a perturbation to the acoustic wave propagation and prevents the radiation of the acoustic field in the surrounding media, a condition which would induce excessive insertion losses. Since the acoustic wave wavelength is of the order of, assuming an acoustic velocity about 3500 m/s, 35 to 7 μm between 100 and 500 MHz, typical film thicknesses will be in the sub-micrometer range.

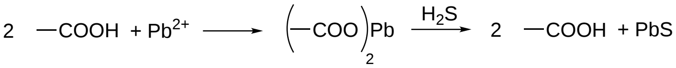

Fig. 2. Sensing principle of H_2S by lead acetate. Lead acetate is colourless while PbS is a black solid.

The organic layer holds the chemical function designed to selectively detect the targeted compound. Our selection, for detecting hydrogen sulfide, is to use the selective affinity of sulfur for noble metals, with the initial insight coming from the classical colorimetric hydrogen sulfide method of monitoring lead acetate soaked strips of paper: lead acetate reacts with hydrogen sulfide to create lead sulfide nanoparticles which make the paper color switch from white to black (Fig. 2). Hence, designing an organic matrix holding lead, or any other metal selectively reacting with sulfur such as gold [21], zinc or copper [22], ions will provide the selective sensing capability.

II. SENSOR FUNCTIONALIZATION

Having selected the development strategy of functionalizing a polymer with noble metal ions selectively reacting with the sulfur atom of hydrogen sulfide, the problem of reproducibly and homogeneously spreading the polymer on the surface of the sensor needs to be tackled. Collective, wafer scale fabrication provides cost effective means of reproducible sensor surface functionalization. Classical surface functionalization techniques include self assembled (mono)layers, drop casting, spraying or spin coating. The latter is arguably the most common technique in cleanroom processing: a substrate is spun at fast rotation speed for the centrifugal force to spread the polymer dissolved in a solvent over the surface of the sensor.

In order to be compatible with the spin coating process, the polymer formulation must be tuned for the viscosity to match typical spin coating conditions. As an example of this approach, the various formulations of Microposit Shipley S1800 or Microchemicals AZ1500 photoresist families are given with varying solvent concentrations for a given thickness to be reached at a given rotation speed of the wafer. Despite the lack of centrifugal force homogeneity along the wafer radius, excess resist is ejected from the spinning wafer and surface tension homogenizes the thickness on the central part of the wafer. Once the polymer has been mixed with the noble metal ion compound, reaching the appropriate viscosity then requires adding the appropriate amount of solvent to the mixture (Fig. 3). This example illustrates one functionalization strategy, in which the lead-containing compound is added to MicroChem's SU8 photoresist, well known for its excellent spin-coating design and the ability to address a wire range of thicknesses,

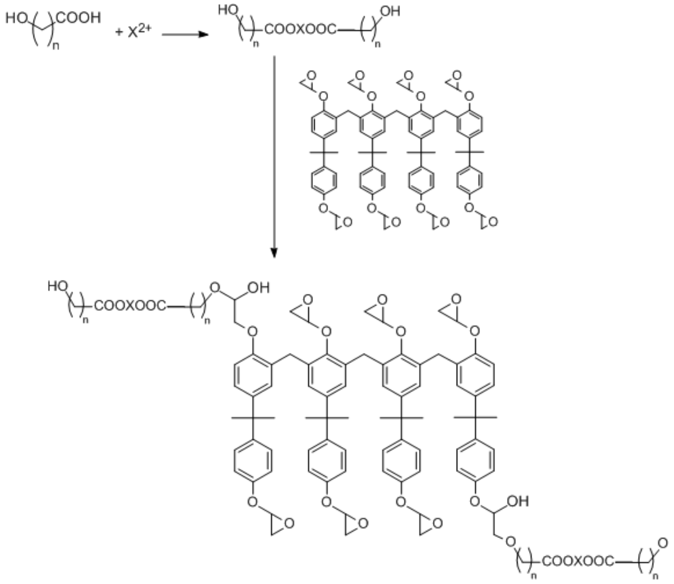

Fig. 3. Inserting the lead ion in a polymer formulation suitable for spin-coating.

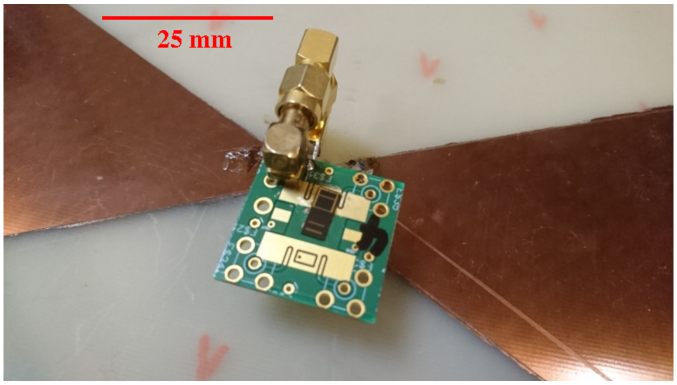

Fig. 4. Diced chip assembled on a printed circuit board and connected to a bowtie antenna for wireless measurement. The total antenna length (no shown) is 60 cm. The printed circuit board dimensions are 25×25 mm^2, the sensor chip is 10×4 mm^2, compatible with 13×7 mm^2 Kyocera ceramic packages.

from sub-micrometer thickness to several hundred micrometer thick layers [1] for high aspect ration structure patterning. Other formulations with lighter epoxy containing molecules have provided better sensitivity of the final transducer thanks to a more favorable lead to carbon weight ratio.

The bigger the sensor with respect to the sensing area, the more homogeneous the layer and the smaller the effect of capillarity on the sides of the sensor: we have functionalized sensors patterned on four-inch lithium niobate wafers – a piezoelectric substrate selected for its strong electromechanical coupling coefficient – *before* dicing the individual 10×4 mm^2 chips, yielding more than 150 sensors for each cleanroom run, making the process cost effective through high volume production (Fig. 4).

Having homogeneously spread the sensing film over the sensor surface, initial characterizations are performed in a controlled environment using a network analyzer wired to the sensor. Hydrogen sulfide is generated by reacting FeS+2 HCl$\rightarrow$Cl$_2$+H$_2$S and the resulting gas fills syringes for storage. During the experiment, the sensing surface is exposed to this air flow saturated in hydrogen sulfide, under ambient conditions of temperature and pressure. The evolution of the phase of the acoustic signal monitored during the reaction is shown in Fig. 5. The baseline for the first 180 s slowly rises due to temperature stabilization of the sensor chip under the fume hood. Then, the exposure to hydrogen sulfide at date 180 s is clearly seen as a phase shift indicating the acoustic wave slowing down due to the mass loading of the gas reacting with the lead ions. Considering our 2×2 mm^2 sensing area, the 50° phase shift is consistent with typical values observed for absorption processes on SAW devices: [23] demonstrates such a phase variation for different acoustic propagation modes when loading the sensor with 50 to 250 ng/mm^2 Au. Assuming this gravimetric sensitivity is representative of the behaviour of our lithium niobate device and considering that about 68 ng/mm^2 (to simplify the numerical application) was added to the layer mass during the hydrogen sulfide (34 g/mol molar weight) exposure, the 250 nm-thick polymer layer (as measured using a profiler after spin coating) has absorbed 2 nmol in $250 \cdot 10^{-9}$ cm^3 or $8 \cdot 10^{-3}$ mol/cm^3. This reactive site density is consistent with a resist of about 250 g/mol molar weight, and a density of the order of 2 g/cm^3, functionalized with a single lead site per monomer molecule, providing $2/250 = 8 \cdot 10^{-3}$ mol/cm^3 reactive sites.

As the hydrogen sulfide reaction is not reversible, the sensor integrates the cumulative gas concentration to which the transducer is exposed between two measurement sequences, hence providing some sort of memory effect of the sensor even if the transducer response is not continuously monitored.

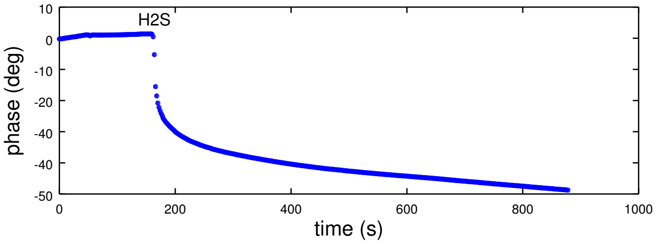

Fig. 5. Sensor response when exposed to hydrogen sulfide.

III. SENSOR INTERROGATION

Having designed a cooperative target whose echo delay – defined as the acoustic wave propagation path length divided by the varying acoustic velocity under varying targeted compound concentration – is dependent on the chemical element concentration, we must address the ability to probe the sensor response using a GPR. Time delay is best measured as a phase shift: in order to assess the detection limit of the

---

[1] http://www.microchem.com/pdf/SU-82000DataSheet2000_5thru2015Ver4.pdf, retrieved January 2017

sensor and the associated measurement system, the baseline stability must be measured. Indeed, any drift of the baseline due to the measurement electronics or transducer operating conditions will prevent the detection of a chemical compound concentration variation. Such a measurement was performed with a commercial Malå ProEx GPR unit operating with 200 MHz unshielded or 250 MHz shielded antennas.

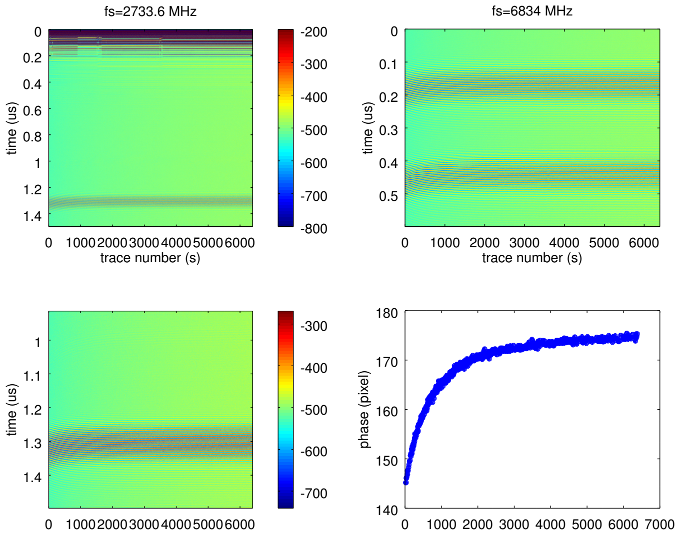

Fig. 6. Acoustic delay line measurement in a constant environment using a commercial GPR (Malå ProEx). Top left is the radargram ranging from 0 to 1.5 μs, with the first echo from the delay line visible at the bottom of the chart. Bottom left is a zoom on this low sampling rate acquisition on the first echo of the delay line. Top right is an acquisition focusing solely on the first two echos of the delay line, separated by about 300 ns. Bottom right is the delay between the first and second echo, expressed in sampling periods.

A major disappointment when replacing the network analyzer (Fig. 5) with a GPR unit (Fig. 6) was to observe a tremendous drift of the phase during the warm up of the interrogation unit [24], lasting up to several hours (Fig. 6). This acquisition was completed using our custom opensource Proexgprcontrol software, available at https://sourceforge.net/projects/proexgprcontrol. Similar results were obtained using the proprietary Groundvision software provided by Malå, so the cause of the drift is not the software but the stroboscopic timing generator [25]: indeed, the emitted pulse is observed to always be generated at the same time (emitted pulse time as observed on the radargram), and while the delay line remains in a constant environment (temperature variation less than 1°C during the two-hour experiment), the received echoes drift. Our software, dedicated to subsurface sensor measurement, implements two measurement windows, one focusing on the shallow subsurface environment (here used in the left column of Fig. 6), and a secondary window focusing on the sensor response (here used in the right column of Fig. 6). The long time window including the emitted pulse as well as the first sensor echo (Fig. 6, left) was recorded to check that the emitted pulse does not drift over time: this low sampling rate is needed to measure over the long duration (1.4 μs including the first echo delayed by the acoustic delay line sensor) before the sensor response is observed, due to the limited number of samples the GPR unit can record. The drift analysis is performed on the data displayed on the right, in which the delay between two echoes returned by the sensor – to compensate for any variation of the measurement unit to sensor distance (not used here in the static setup) – is computed and displayed in units of sampling period – here 146 ps. A drift of 30 pixels lasts 4.4 ns or nearly one period of the 200 MHz emitted pulses. While negligible for subsurface distance measurement – this drift accounts for 1.5% of the 300 ns delay between adjacent echoes – it prevents any fine acoustic velocity analysis of the sensor response to recover the gas concentration. The drift of 4.4 ns at 190 MHz, the central operating frequency of the acoustic delay line, accounts for $360 \times 4.4 \times 0.190 \simeq 300°$ phase drift. The phase shift associated with the acoustic velocity variation due to gas absorption in the polymer was measured as 50°: the baseline drift is six times larger than the observed signal variation due to an atmosphere saturated in the gas to be detected. Were the drift removed, the baseline standard deviation would exhibit acceptable signal to noise ratio, with a phase standard deviation computed on samples dated 845 s to the end and subtracted with a second order polynomial fit, of 0.365 sampling periods or 53 ps or 3.6° or one fifth of the observed signal variation due to gas absorption in the sensing polymer layer. Such a result is obtained with no stacking, one measurement every second and no sliding average.

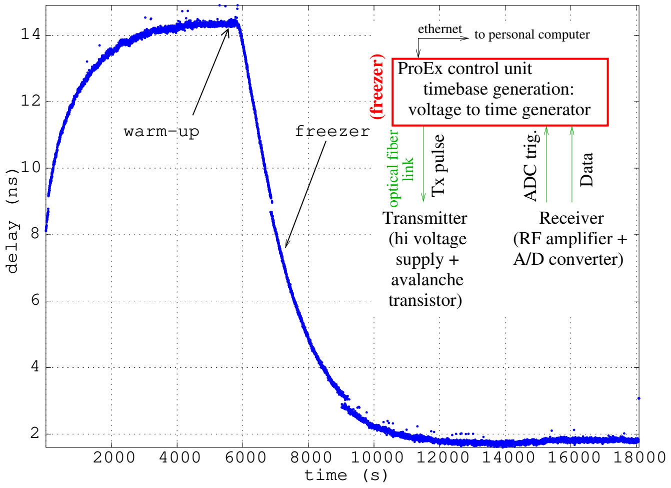

Fig. 7. Demonstration of the stroboscopic timebase generator as the source of the sampling rate drift: the emitter and transmitter (250 MHz unshielded antenna set) are kept at room temperature while the ProEx control unit, which includes the voltage to time pulse delay generator, is first left to warm up before being inserted, at date 6000 s, in a freezer (−18°C) and left to cool until the end of the experiment. The inversion of the drift rate demonstrates that the ProEx control unit, whose only analog function is the timebase generator, is the source of the problem. The experiment was performed with the control unit powered by a stabilized laboratory power supply. The two phase jumps at 7000 and 9000 s are due to imperfect unwrapping.

Fig. 7 demonstrates that the stroboscopic timing generator is the cause of the drift: two voltage ramps at different rates feed a comparator whose output defines the emission pulse time and sampling time, as classically implemented in a voltage to time generator. The slow ramp, defining the sampling rate and sampling time range, is generated by a digital to analog converter whose output runs through an operational amplifier. Not only is this operational amplifier observed to excessively heat – above 50°C when the ProEx control unit is kept at room temperature – inducing an internal offset (the datasheet hints at a 12 μV/°C temperature offset for this part) and hence a timebase drift, but most significantly cooling the whole control unit reverses the drift trend. We have observed that cooling this particular component alone was sufficient to reverse the cause of the drift. Dynamic temperature control or compensation is under investigation. Here again, a drift of ±6 ns or 410 angle degrees at 190 MHz is observed, consistent with previous measurements.

IV. LIQUID PHASE COMPATIBILITY

All measurements so far have been performed on acoustic delay lines patterned on lithium niobate, a strongly coupled piezoelectric substrate used to generate a Rayleigh wave in our application. Rayleigh waves are surface acoustic wave with an elliptical polarization, hence exhibiting an out of plane displacement component and hence the capability to radiate acoustic power in a surrounding fluid through progressive pressure waves. Such coupling induces excessive acoustic losses and the sensor is not usable in liquid phase. In order to prevent such acoustic wave coupling with the surrounding liquid, the classical approach is to use a shear wave, as exhibited by quartz in a Love mode configuration, or lithium tantalate [26] in the p-SAW (pseudo-surface acoustic wave [27]) configuration (Fig. 8) in which the wave is prevented from radiating into the bulk of the substrate by an electically conducting coating slowing down the wave and confining its propagation to the surface. While the latter [28], [29], [30] has been shown to exhibit lower gravimetric sensitivity than a quartz-based Love mode device [23], an additional constraint is packaging to insulate the electrodes converting the incoming electromagnetic wave to an acoustic wave.

Not only do the electrodes need to be insulated against resistive short-circuit, a task easily completed by a thin passivation layer, but also against capacitive short circuit. Indeed, coating the transducer electrodes with water increases the sensor environment permittivity from 1 (air) to 80 (water), and the parasitic capacitance short circuiting the electrodes rises by this factor as well. When using a substrate with low permittivity such as quartz ($\varepsilon_r \simeq 5$), the incoming electromagnetic energy is diverted from reaching the piezoelectric substrate towards the surrounding liquid when the electrodes overlaying medium is replaced from air to water. On the other hand, a substrate with a high permittivity is hardly affected by the replacement of the low permittivity air with the high permittivity water: a fraction of the incoming electromagnetic wave will nevertheless go in the fluid, but a sufficient fraction of the incoming power will couple with the high-permittivity substrate and become converted to an acoustic wave. One material comes out has propagating a shear wave, exhibiting high permittivity and strong electromechanical coupling: lithium tantalate.

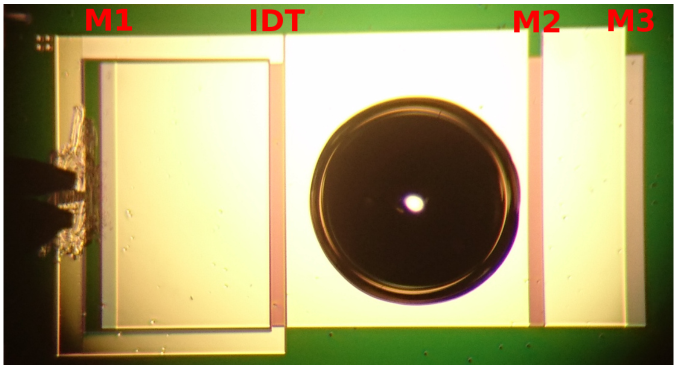

Fig. 8. Acoustic reflective delay line patterned on a lithium tantalate device. From left to right: contact pads, first mirror, first sensing area coated with metal, interdigitated transducers, second sensing area coated with metal and covered with a drop of water, second mirror, third sensing area coated with metal and third mirror. The probe tips can be seen to have scratched the photoresist guiding layer: due to the high pyroelectric property of lithium tantalate making the substrate challenging to process, the pad opening lithography step was not performed in the cleanroom and the whole wafer is coated with a 500 nm thick S18 photoresist layer.

Such a substrate has been used in several investigations focusing on chemical compound detection in liquid phase when the microfluidic handling for preventing the fluid from reaching the electrodes of a low permittivity substrate (quartz) is given up. We have fabricated lithium tantalate acoustic delay lines with delays and operating frequencies similar to those found on the lithium niobate devices used previously, and coated the transducer with a thin organic layer to prevent resistive short circuit and confine the acoustic wave to the surface in a Love mode strategy. Additionally, the acoustic wave was prevented from radiating towards the bulk of the piezoelectric substrate by coating the sensing area with a metallic layer, thus slowing down the surface acoustic wave and preventing its radiation as a bulk wave which would have induced excessive propagation losses. The photoresist guiding layer is assumed to behave in a way representative of the hydrogen sulfide detection thin film (Fig. 9). Despite losses greater than those observed for a lithium niobate device, the guiding layer thickness and number of electrode pairs in the interdigitated transducer remain to be optimized for reaching the best link budget.

V. CONCLUSION

Ground Penetrating RADAR (GPR) is considered as an interrogation unit for probing passive cooperative targets for measuring sub-surface chemical compound concentration, using a Surface Acoustic Wave transducer approach. We demonstrate a sensor functionalization for detecting hydrogen sulfide in gas phase, and that a commercial GPR unit exhibits unsuitable stability to finely measure the phase of the returned echoes, representative of gas concentration. Additionally, we extend the analysis towards a sensor design compatible with compounds located in liquid phase. We thus demonstrate

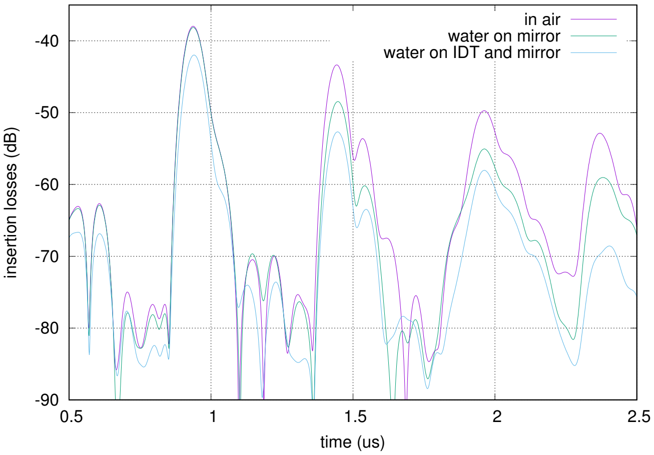

Fig. 9. Acoustic response, in the time domain, of the reflective delay echoes when the sensor is exposed to air, the second sensing area is coated with a drop of water (as seen on Fig. 8), and the second sensing area as well as the interdigitated transducers are coated with water.

the design of lithium-tantalate devices compatible with GPR interrogation, exhibiting low insertion loss variation when electrodes, sensing areas and mirrors are coated with water, and yet functionalized with an organic thin film for selective chemical detection.

ACKNOWLEDGMENT

The Malå ProEx GPR control unit acquisition was funded by a grant from the Franche-Comté district. The hydrogen sulfide detection project was funded in the framework of the CITEPH 25-2014 grant provided by Total SA (Paris, France) & Entrepose Contracting (Colombes, France). This work was partly supported by the French RENATECH network and its FEMTO-ST technological facility. Common research activities between SENSeOR SAS and FEMTO-ST are supported through the PhASES joint laboratory. Malå has been helpful in supporting this investigation by lending a ProEx control unit to double check the timebase drift issue.

REFERENCES

[1] J.-M. Friedt and A. Hugeat, "A low cost approach to acoustic filters acting as gpr cooperative targets for passive sensing," in *IEEE 8th International Workshop on Advanced Ground Penetrating Radar (IWAGPR)*, 2015, pp. 1–4.

[2] J.-M. Friedt, "Passive cooperative targets for subsurface physical and chemical measurements," in *GPR2016*, Hong Kong, 2016.

[3] V. P. Plessky and L. M. Reindl, "Review on SAW RFID tags," *IEEE transactions on ultrasonics, ferroelectrics, and frequency control*, vol. 57, no. 3, pp. 654–668, 2010.

[4] L. Reindl, C. Ruppel, A. Kirmayr, N. Stockhausen, M. Hilhorst, and J. Balendonck, "Radio-requestable passive SAW water-content sensor," *IEEE Transactions on Microwave Theory and Techniques*, vol. 49, no. 4, pp. 803–808, 2001.

[5] F. Bender, F. Josse, R. Mohler, and A. Ricco, "Design of SH-surface acoustic wave sensors for detection of ppb concentrations of BTEX in water," in *2013 Joint UFFC, EFTF and PFM Symposium*, 2013, pp. 628–631.

[6] F. Bender, R. Mohler, A. Ricco, and F. Josse, "Identification and quantification of aqueous aromatic hydrocarbons using SH-surface acoustic wave sensors," *Anal. Chem*, vol. 86, no. 3, pp. 1794–1799, 2014.

[7] W. Wang, K. Lee, T. Kim, I. Park, and S. Yang, "A novel wireless, passive CO_2 sensor incorporating a surface acoustic wave reflective delay line," *Smart Mater. Struct.*, vol. 16, pp. 1382–1389, 2007.

[8] W. Wang and S. He, "A Love wave reflective delay line with polymer guiding layer for wireless sensor application," *Sensors*, vol. 8, pp. 7917–7929, 2008.

[9] W. Wang, C. Lim, L. Lee, and S. Yang, "Wireless surface acoustic wave chemical sensor for simultaneous measurement of CO_2 and humidity," *J. Micro/Nanolith. MEMS MOEMS*, vol. 8, no. 3, p. 031306, 2009.

[10] I. Leonte, M. Hunt, G. Sehra, M. Cole, J. Gardner, H. S. Noh, and P. Hesketh, "Towards a wireless microsystem for liquid analysis," in *IEEE Trans*, 2004.

[11] J. Perng, W. Hunt, and P. Edmonson, "Development of a shear horizontal SAW RFID biosensor," in *IEEE SENSORS Conference*, 2007.

[12] F. Hassani, S. Ahmadi, C. Korman, and M. Zaghloul, "A SAW-based liquid sensor with identification for wireless applications," in *IEEE International Symposium on Circuits and Systems - ISCAS*, 2010, pp. 2023–2026.

[13] H.-K. Oh, W. Wang, K. Lee, C. Min, and S. Yang, "The development of a wireless love wave biosensor on 41° YX $LiNbO_3$," *Smart Mater. Struct.*, vol. 18, p. 025008, 2009.

[14] P. A. Hessel, F. A. Herbert, L. S. Melenka, K. Yoshida, and M. Nakaza, "Lung health in relation to hydrogen sulfide exposure in oil and gas workers in Alberta, Canada," *American journal of industrial medicine*, vol. 31, no. 5, pp. 554–557, 1997.

[15] T. N. Nazina, E. P. Rozanova, and S. I. Kuznetsov, "Microbial oil transformation processes accompanied by methane and hydrogen-sulfide formation," *Geomicrobiology Journal*, vol. 4, no. 2, pp. 103–130, 1985.

[16] S. Myhr, B.-L. Lillebø, E. Sunde, J. Beeder, and T. Torsvik, "Inhibition of microbial H_2S production in an oil reservoir model column by nitrate injection," *Applied microbiology and biotechnology*, vol. 58, no. 3, pp. 400–408, 2002.

[17] C. Ren, D. Liu, Z. Bai, and T. Li, "Corrosion behavior of oil tube steel in simulant solution with hydrogen sulfide and carbon dioxide," *Materials chemistry and physics*, vol. 93, no. 2, pp. 305–309, 2005.

[18] F. Osorio and J. Torres, "Biogas purfication from anaerobic digestion in a wastewater treatment plant for biofuel production," *Renewable Energy*, vol. 34, pp. 2164–2171, 2009.

[19] L. Hayes, "Control of hydrogen sulfide emissions associated with wasterwater treatment plants," *Pract. Period. Hazard. Toxic Radioact. Waste Manage.*, vol. 3, pp. 35–38, 1999.

[20] J. F. Vetelino, R. Lade, and R. Falconer, "Hydrogen sulfide surface acoustic wave gas detector," *IEEE transactions on ultrasonics, ferroelectrics, and frequency control*, vol. 34, no. 2, pp. 156–161, 1987.

[21] S. Mubeen, T. Zhang, N. Chartuprayoon, Y. Rheem, A. Mulchandani, N. Myung, and M. Deshusses, "Sensitive detection of H_2S using gold nanoparticles decorated SWNTs," *Anal Chem.*, vol. 82, no. 1, pp. 250–257, 2010.

[22] J. M. Davidson, C. M. Grant, and R. E. Winpenny, "Fast reaction of solid copper (i) complexes with hydrogen sulfide gas," *Industrial & engineering chemistry research*, vol. 40, no. 13, pp. 2982–2986, 2001.

[23] K. Mitsakakis, A. Tsortos, J. Kondoh, and E. Gizeli, "Parametric study of SH-SAW device response to various types of surface perturbations," *Sensors and Actuators B*, vol. 138, pp. 408–416, 2009.

[24] J.-M. Friedt, "Passive cooperative targets for subsurface physical and chemical measurements: a systems perspective," *IEEE Geoscience and Remote Sensing Letters*, 2017, submitted.

[25] B. Johansson, "Ground penetrating radar array and timing circuit," 2002, patent US 6496137.

[26] T. Kogai, H. Yatsuda, and S. Shiokawa, "Improvement of liquid-phase SH-SAW sensor device on 36° Y-X $LiTaO_3$ substrate," in *IEEE International Ultrasonics Symposium Proceedings*, 2008, pp. 98–101.

[27] D. Morgan, *Surface acoustic wave filters: With applications to electronic communications and signal processing*. Academic Press, 2010.

[28] F. Martin, M. Newton, G. McHale, K. Melzak, and E. Gizeli, "Pulse mode shear horizontal-surface acoustic wave (SH-SAW) system for liquid based sensing applications," *Biosensors and Bioelectronics*, vol. 19, pp. 627–632, 2004.

[29] A. Malave, U. Schlecht, T. Gronewold, M. Perpeet, and M. Tewes, "Lithium tantalate surface acoustic wave sensors for bio-analytical applications," in *IEEE Sensors*, Daegu, Korea, October 22-25 2006, pp. 604–607.

[30] J. Brookes, R. Bufacchi, J. Kondoh, D. Duffy, and R. McKendry, "Determining biosensing modes in SH-SAW device using 3D finite element analysis," *Sensors and Actuators B*, vol. 234, pp. 412–419, 2016.